2021-07-06

Microtubule disruption upon CNS damage triggers mitotic entry via TNF signaling activation

Barros, Claudia

10.1016/j.celrep.2021.109325
Cell Reports
Elsevier (Cell Press)

Cell Reports

Article

Microtubule disruption upon CNS damage triggers mitotic entry via TNF signaling activation

Graphical abstract

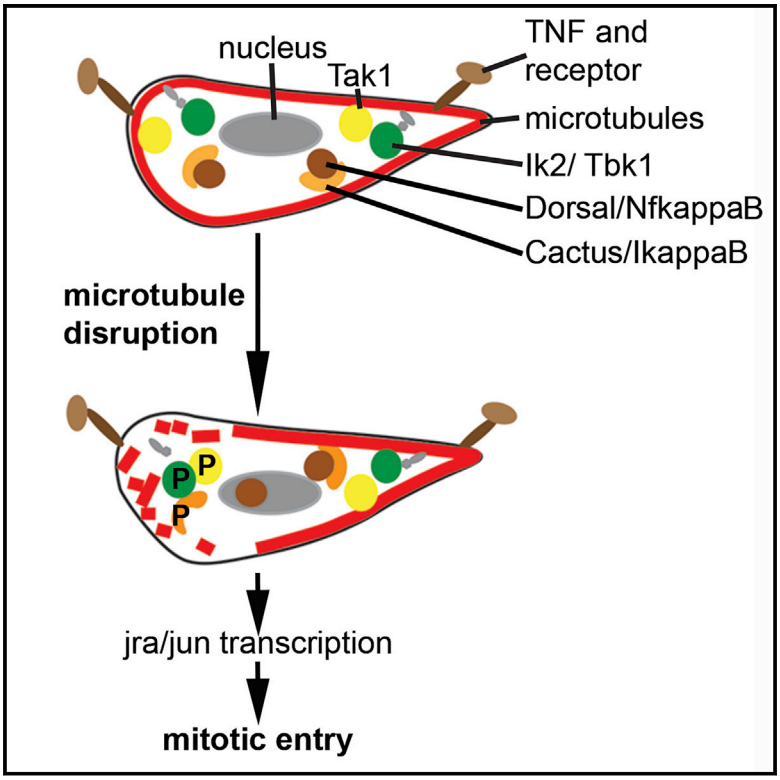

Authors

Claudia S. Barros, Torsten Bossing

Correspondence

torsten.bossing@plymouth.ac.uk

In brief

Barros and Bossing show that TNF signaling kinases Tak1 and Ik2 are activated upon microtubule disruption, resulting in Dorsal nuclear localization, Jun expression, and entry into mitosis of *Drosophila* embryonic midline cells. Tak1 and Tbk1/Ik2 activation is also seen in the subiculum of Alzheimer's brain neurons co-localizing with diseased Tau.

Highlights

- Microtubule disruption at *Drosophila* ventral midline activates TNF signaling
- Phosphorylation of TNF signaling kinases Tak1 and Ik2 results in mitotic entry
- Expression of human Tau triggers Tak1 activation and mitosis at the ventral midline
- Activated Tak1 and Tbk1/ Ik2 colocalize with diseased Tau in Alzheimer's brain neurons

Barros & Bossing, 2021, Cell Reports *36*, 109325
July 6, 2021
https://doi.org/10.1016/j.celrep.2021.109325

CellPress

Cell Reports

CellPress
OPEN ACCESS

Article

Microtubule disruption upon CNS damage triggers mitotic entry via TNF signaling activation

Claudia S. Barros[1] and Torsten Bossing[1,2,*]
[1]Peninsula Medical School, Faculty of Health, University of Plymouth, John Bull Building, 16 Research Way, Plymouth PL6 8BU, UK
[2]Lead contact
*Correspondence: torsten.bossing@plymouth.ac.uk
https://doi.org/10.1016/j.celrep.2021.109325

SUMMARY

Repair after traumatic injury often starts with mitotic activation around the lesion edges. Early midline cells in the *Drosophila* embryonic CNS can enter into division following the traumatic disruption of microtubules. We demonstrate that microtubule disruption activates non-canonical TNF signaling by phosphorylation of TGF-β activated kinase 1 (Tak1) and its target IkappaB kinase (Ik2), culminating in Dorsal/NfkappaB nuclear translocation and Jra/Jun expression. Tak1 and Ik2 are necessary for the damaged-induced divisions. Microtubule disruption caused by Tau accumulation is also reported in Alzheimer's disease (AD). Human Tau expression in *Drosophila* midline cells is sufficient to induce Tak1 phosphorylation, Dorsal and Jra/Jun expression, and entry into mitosis. Interestingly, activation of Tak1 and Tank binding kinase 1 (Tbk1), the human Ik2 ortholog, and NfkappaB upregulation are observed in AD brains.

INTRODUCTION

Tissue damage repair encompasses processes from wound closure to the complete replacement of a lost organ (Bely and Nyberg, 2010). Repair is often initiated by mitotic activation of the cells adjacent to the damage, and increased proliferation may be required for wound closure and replacement of lost tissue (Ricci and Srivastava, 2018). A wide range of signaling pathways, including WNT, bone morphogenic protein (BMP), transforming growth factor β (TGF-β), Hippo, mTor, and neuregulin signaling, activate and coordinate repair (Forbes and Rosenthal, 2014; Ricci and Srivastava, 2018). Cell signaling can induce divisions in cells adjacent to the wound, either through dedifferentiation or via reactivation of dormant stem cells (Ricci and Srivastava, 2018). Reactivation of neural stem cells is a major response to injuries in the mammalian central nervous system (CNS). However, the repair capacity of neural stem cells in mammals is limited and the mechanisms of reactivation remain largely unknown (Chang et al., 2016; Ruddy and Morshead, 2018). We have shown that damage at the ventral midline of the embryonic *Drosophila* CNS causes midline cells adjacent to the wound to enter into mitosis and to replace lost cells. Interestingly, the trigger for these injury-induced divisions is the disruption of the microtubule cytoskeleton. Chemical, mechanical, and genetic disruption of microtubules, but not actin depolymerization, drives midline cells into mitosis (Bossing et al., 2012). Here, we show that microtubule disruption activates the phosphorylation of TGF-β activated kinase 1 (Tak1) and its downstream target IkappaB kinase (Ik2), which is sufficient to trigger mitosis in midline cells. This activation is dependent on tumor necrosis factor (TNF) signaling and can be inhibited by activation of the Jun kinase (JNK) cascade. We also found that midline expression of human Tau proteins, which have previously been reported to interfere with the integrity of microtubules (Cowan et al., 2010), is sufficient to activate mitosis, Tak1, Dorsal, and Jra/Jun expression. Interestingly, we detect phosphorylation of Tak1 and the human Ik2 ortholog, Tank binding kinase 1 (Tbk1), in the mature neurons of Alzheimer's disease (AD) brains but only rarely in age-matched controls. Tak1 phosphorylation and expression of the human ortholog of *Drosophila* Dorsal, NfkappaB (also known as p65), are both high in AD brains and linked to sites of diseased Tau accumulation. In addition, pTbk1 expression often colocalizes with abnormal activation of the mitotic marker Ki67. The expression of mitotic markers in mature neurons has previously been linked to cell death (Copani et al., 1999, 2001; Frade and Ovejero-Benito, 2015; Hisanaga and Endo, 2010; Husseman et al., 2000; Marlier et al., 2020; Park et al., 2007; Tian et al., 2009). Accordingly, in AD brains, pTbk1 expression shows high colocalization with the cell death marker cleaved caspase 3. Our findings using *Drosophila* demonstrate that microtubule disruption activates TNF signaling components initiating damage-induced cell division in the CNS, a mechanism that may be conserved through evolution.

RESULTS

Injury at the ventral midline activates Dorsal/NfkappaB signaling

We previously showed that the removal of partially determined but not yet differentiated ventral midline (Bossing and Brand, 2006) cells from the embryonic *Drosophila* CNS activates mitosis at the wound site, resulting in the replacement of damaged cells. Single-cell transcriptional profiling of midline cells revealed that microtubule disruption triggers mitosis and Jun transcription,

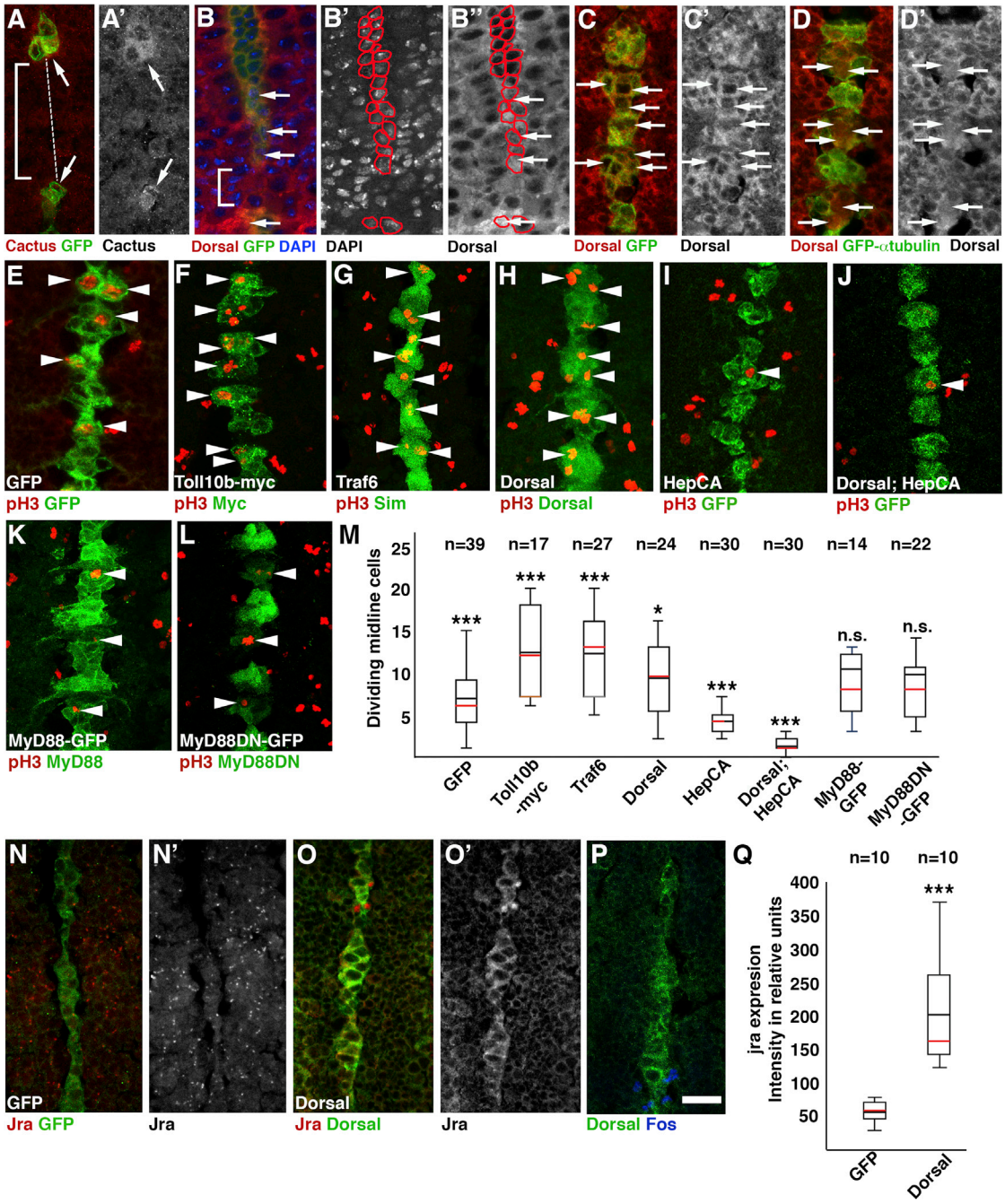

Figure 1. Dorsal/NFkB signaling is upregulated in the midline following damage and drives mitosis

(A) Midline cells (green) were removed (bracket marks damage, dashed line marks midline) from early embryos (stage 10). Midline cells adjacent to the lesion upregulate Cactus/NFKBIA (red, arrows). (A′) shows Cactus only. Genotype, *simG4>myrGFP*. Embryos were fixed 70 min after ablation.

(B) After damage (bracket) to midline cells (green), cells adjacent to the wound exhibit nuclear translocation of Dorsal/NfkappaB (red, arrows). Note nuclear entry of dorsal proximal but not distal to the damage. Nuclei encircled red. (B′) shows nuclei only; (B′′) shows dorsal only. Genotype, *simG4>myrGFP*. Embryos were fixed 10 min after ablation.

(C and D) Midline cells expressing membrane GFP (green) exclude dorsal (red) from their nuclei (arrows, C), but midline expression of GFP-α-tubulin (green) results in nuclear translocation of dorsal (arrows, d). (C′) and (D′) show dorsal only. Genotype, *simG4>myrGFP,* nuclear Dorsal x = 1.4 ± 0.4 cells/segment, n = 8; *simG4>GFP-α-tubulin62E*, x = 3.19 ± 0.73 cells/segment, n = 13.

(E–L) Targeted expression of Toll/TNF pathway components in midline cells. Targeted protein indicated at bottom of each image (white). Midline cells, green; dividing cells, red (anti-phospho histone H3 [S10], pH3). Expression of a constitutive active form of the Toll receptor (Toll10b; F), of Traf6 (G) and Dorsal (H) increase midline cell divisions in undamaged midline cells (stage 13). Expression of a constitutively active form of Hep (HepCA) reduces midline cell divisions (I)

(legend continued on next page)

which is essential for the damage-induced divisions (Bossing et al., 2012).

Profiling also shows an activation of Cactus/NFkappaB inhibitor alpha (NFKBIA) transcription. Immunohistochemistry confirms increased Cactus expression in cells adjacent to the damage (Figures 1A and 1A′). Cactus is upregulated 70 min after damage either at one (3/5 embryos) or both wound edges (2/5 embryos; Figures 1A and 1A′). Cactus, the *Drosophila* ortholog of the human NFKBIA, is the penultimate signaling component in the widely conserved Toll and TNF signaling cascades (Hayden and Ghosh, 2004). In the cytoplasm, Cactus binds the transcription factor Dorsal/NfkappaB. Upon signal activation, Cactus is targeted for degradation and Dorsal is released into the nucleus to activate its targets (Hayden and Ghosh, 2004). We can detect Dorsal in the nucleus of midline cells at the wound site 20 min after damage (18/32 embryos; Figure 1B). Most embryos (15/18) show nuclear Dorsal only at one side of the injury. Midline targeted expression of α-tubulin mimics external damage, disrupting microtubules and activating midline cell divisions (Bossing et al., 2012). The expression of α-tubulin in the midline also drives Dorsal into the nucleus (Figures 1C to 1D′). We conclude that external and internal damage to microtubules activates the transcription factor Dorsal in midline cells.

Dorsal activation increases midline cell divisions and upregulates Jra expression

We tested whether Dorsal activation stimulates mitosis by expressing different upstream signaling components in ventral midline cells. Activating Dorsal signaling by the expression of a constitutive active myc-tagged Toll receptor isoform (Hu et al., 2004), the signal transducer Traf6 (Shen et al., 2001), or Dorsal itself (Huang et al., 2005) stimulates mitosis in midline cells immediately after germband shortening (stage 13; Figures 1E–1H and 1M). In contrast, the expression of a constitutively active form of Hemipterous (HepCA)/JNKK (Figure 1I), a component of JNK signaling frequently activated in wound healing (Martín and Morata, 2018), represses midline cell divisions even in the presence of midline targeted Dorsal (Figures 1J and 1M). No increase in cell divisions results from midline expression of a GFP-tagged full-length dMyD88-GFP, a Toll signaling transducer, or a GFP-tagged truncated dMyD88-GFP (MyD88DN) comprising the first 236 amino acids (aa) of the N terminus and acting as a dominant inhibitor of the Toll pathway (Horng and Medzhitov, 2001) (Figures 1K and 1M).

Damage at the ventral midline induces the expression of Jra, the *Drosophila* Jun ortholog, which is essential for the mitotic activation of cells at the wound site (Bossing et al., 2012). Interestingly, midline targeted expression of Dorsal not only prompts cell division but also initiates Jra expression (Figures 1N–1O′ and 1Q). Neither damage nor Dorsal activation upregulate Fos expression (Figure 1P), arguing against an involvement of the activator protein 1 (AP-1) complex (Bejjani et al., 2019) in midline damage repair.

We conclude that Dorsal activation in midline cells triggers Jra transcription and is able to stimulate midline cell division even without injury.

TNF signaling is required for mitotic activation after midline damage

Since Dorsal activation is able to stimulate midline divisions, we tested whether Toll or TNF signaling is upstream in damage repair at the midline. We damaged the ventral midline in living embryos (stage 10) by removing cells with a microcapillary. Embryos were fixed 45 min after the damage and stained for the mitotic marker phospho (S10) histone H3 (pH3). Indistinguishable from wild-type embryos (61%), damage in embryos with impaired Toll signaling (*rhoG4>MyD88DN*) trigger mitosis in ~60% of samples (Figures 2A, 2B, and 2G). However, partial loss of Eiger (Egr), the *Drosophila* TNF ortholog, in heterozygotes or by the expression of RNAi reduces mitotic activation after damage to 47% and 33%, respectively (Figure 2G). Complete loss of Egr reduces mitotic induction at the wound to 9% (Figures 2D and 2G). Tak1 is recruited to the TNF receptor complex after activation (Blonska et al., 2005). In *Tak1* mutants, mitotic activation after damage is severely reduced to 19% (Figures 2E and 2G). We also tested whether functional loss of Wengen (Wgn), the TNF receptor expressed in the embryonic CNS (Kauppila et al., 2003), affects midline repair. In contrast to *egr*, expression of *wgn* RNAi in midline still allows midline repair (53%) (Figures 1F and 1G).

At the time of ablations, Egr is expressed in all midline cells and adjacent ectoderm stripes, colocalizing with Engrailed (En) (Figures S1A and S1B). The removal of midline cells creates gaps in Egr and En at the midline and adjacent ectoderm but does not cause any upregulation of Egr expression at the wound site (Figure S1C).

In conclusion, our results suggest that a non-canonical TNF signaling pathway is upstream of mitotic activation at midline damage sites.

Ik2 phosphorylation (pIk2) is triggered by microtubule disruption

Activation of Tak1 results in the phosphorylation and activation of Ik2, the kinase that phosphorylates Cactus, triggering the nuclear

and suppresses the increased divisions caused by Dorsal expression (J). Midline targeted MyD88 (K) and its dominant-negative isoform, MyD88DN (L), have no effect.

(M) Quantification of midline cell divisions. Wilcoxon rank-sum test. ***$p < 0.001$; *$p < 0.05$. n.s., not significant. Black line, average value; red line, median value. n, number of biological replicas (embryos). Genotypes and averages are GFP, *simG4>myrGFP*, x = 6.82; Toll10b, *simG4>Toll10bmyc*, x = 12.35; Traf6, *simG4>TRAF6*, x = 12.1; Dorsal, *simG4>dorsal*, x = 9.3; HepCA, simG4>HepCA, x = 4.1; Dorsal;HepCA, *simG4>dorsal;HepCA*, x = 1.3; MyD88-GFP, *simG4>MyD88GFP*, x = 11.2; MyD88DN-GFP, *simG4>MyD88DNGFP*, x = 9.8.

(N and O) Dorsal (green, O) but not membrane GFP expression (green, N) activates Jra/Jun (red) expression at the midline (green). (N′) and (O′) show Jra only.

(P) Midline targeted Dorsal is not able to activate Fos expression (blue).

(Q) Quantification of Jra expression. Intensity, integrated density. Wilcoxon rank-sum test. ***$p < 0.001$. Black line, average value; red line, median value. GFP, *simG4>myrGFP*, x = 56.8; Dorsal, *simG4>dorsal*, x = 203.4.

Embryonic stages are 11 (A and B), 13 (C–L), and 12 (N and O). Ventral views, anterior up. Scale bar, 20 μm.

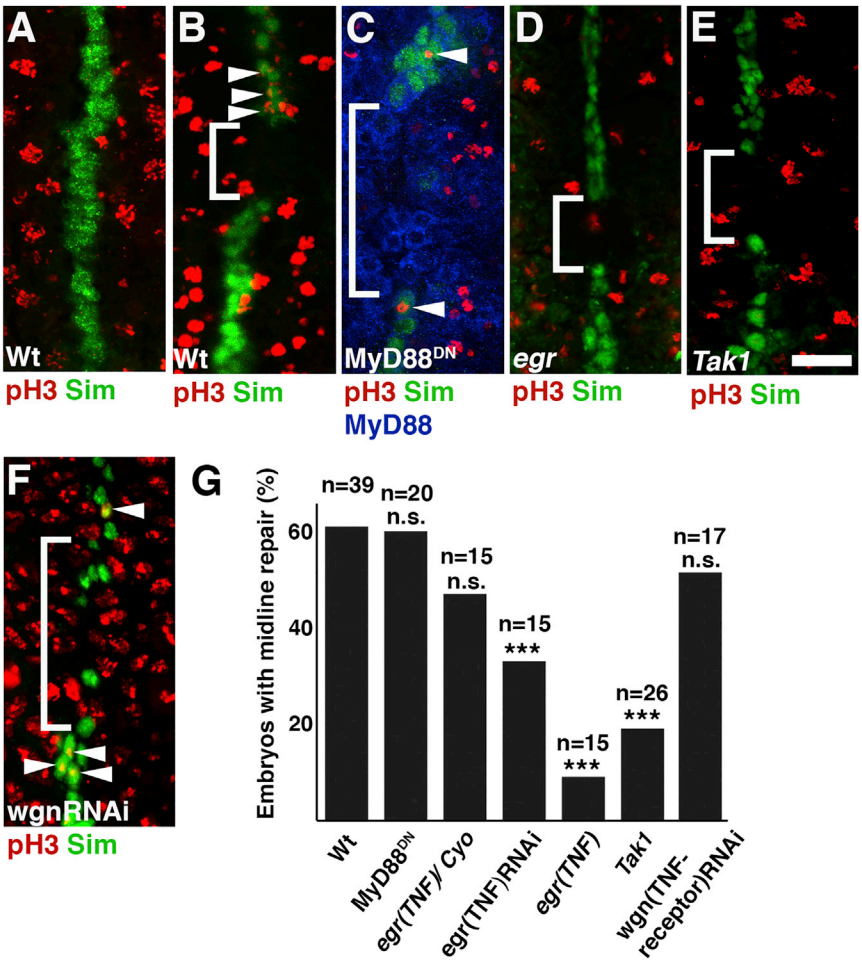

Figure 2. TNF signaling is required for mitotic activation at midline injury sites

(A) In stage 10 embryos, undamaged midline cells (green, anti-Sim) do not divide (red, anti-pH3).

(B) Removal of midline cells (bracket) in stage 10 embryos triggers cell divisions in midline cells next to the lesion (arrowheads).

(C) Extra divisions (red) also occur after midline damage (bracket) in embryos expressing dominant-negative MyD88DN-GFP (blue, anti-GFP) in the ventral ectoderm and midline (green).

(D and E) Loss of Egr/TNF (D) or the kinase Tak1 (E) nearly abolishes midline repair after damage (brackets).

(F) In contrast to midline-targeted *egr* RNAi, midline-expressed *wgn* RNAi does not affect midline repair.

(G) Quantification of midline repair in different genotypes. n, number of biological replicas (embryos). Fisher exact test; n.s., non-significant, ***$p < 0.001$. Genotypes are Wt, *wild-type*; MyD88DN-GFP, *rhoG4>MyD88DN-GFP*; egr(TNF)/Cyo, *egrMI10790/CyO, P{GAL4-twi.G}2.2, P{UAS-2xEGFP}*; egr (TNF)RNAi, *scaG4>P{TRiP.HMC03963}attP40*; *egr(TNF),* egrMI10790; Tak1, *Tak12,* wgn (TNF receptor), *scaG4>P{UAS-wgn.IR}*. Bracket marks area of midline cell removal. Ventral views, anterior up. Scale bar, 20 μm.

entry of Dorsal (Hayden and Ghosh, 2004; Wang et al., 2001). Proteomic analysis has revealed the binding of Tak1 to several α- as well as β-tubulin proteins (Fukuyama et al., 2013). In addition, *Drosophila* Ik2 has been shown to be bound indirectly to microtubules via SpnF and Dynein (Lin et al., 2015). Since microtubule disruption is upstream of midline damage repair (Bossing et al., 2012), we tested whether microtubule disruption also triggers pIk2. In mock-injected embryos (stage 10/11), pIk2 is not detectable in the CNS (Figures 3A, 3A′, and 3C). Injection of the drug vinblastine depolymerizes microtubules and activates pIk2 throughout the CNS (Figures 3B, 3B′, and 3C). In later embryos (stage 13) midline cells show a slightly higher pIk2 than cells in the adjacent CNS (Figures 3D, 3D′, and 3F). At this stage, the expression of α-tubulin at the midline strongly increases pIk2 in segmentally repeated domains (Figures 3E, 3E′, and 3F). Previously, we demonstrated that midline α-tubulin expression reduces endogenous β-tubulin, thereby most likely interfering with microtubule depolymerization (Bossing et al., 2012). To confirm that microtubule depolymerization triggers pIK2 production, we injected Taxol into GFP-α-tubulin-expressing embryos. The stabilization of microtubules reduces pIk2 significantly (Figures 3G–3I). Finally, ~10 min after cell removal, damage sites at the ventral midline exhibit increased pIk2 (Figures 3J and 3K; 6/10 embryos). We conclude that microtubule disruption results in the activation of Ik2.

Ik2 is essential for damage-induced and endogenous midline cell divisions

We show that the disruption of microtubules triggers entry into mitosis and pIk2. To demonstrate the requirement of pIk2 for mitotic activation, we expressed at the midline a dominant-negative Ik2 (Ik2DN; K41A) (Oshima et al., 2006), which no longer can be phosphorylated (*simGal4>Ik2DN*). In contrast to 1% DMSO (Figure 1A), the injection of vinblastine in wild-type embryos initiates divisions in nearly all midline cells in up to four segments around the injection site (Bossing et al., 2012) (Figures 4B, 4B′, and 4D). The midline expression of Ik2DN reduces the number of embryos with mitotic cells after vinblastine injection (Figures 4B–4D). Ik2DN expression also strongly reduces mitosis at damage sites (Figures 4E–4G). We conclude that Ik2 activation is essential for midline divisions caused by microtubule disruption.

To test whether Ik2 can also modulate endogenous midline divisions, we scored mitotic cells in stage 13 embryos expressing midline-targeted full-length Ik2 (Oshima et al., 2006) or Ik2DN (Figures 4H–4J). Raising midline Ik2 levels has no effect on mitosis numbers. Increased expression of Ik2DN reduces, but does not abolish, midline cell divisions (Figure 4N).

Midline expression of α-tubulin increases midline cell divisions (Bossing et al., 2012) (Figures 4K and 4N). Surprisingly, full-length Ik2, which does not alter endogenous midline divisions, reduces midline cell divisions to wild-type levels when expressed together with α-tubulin (Figures 4L and 4N). In contrast,

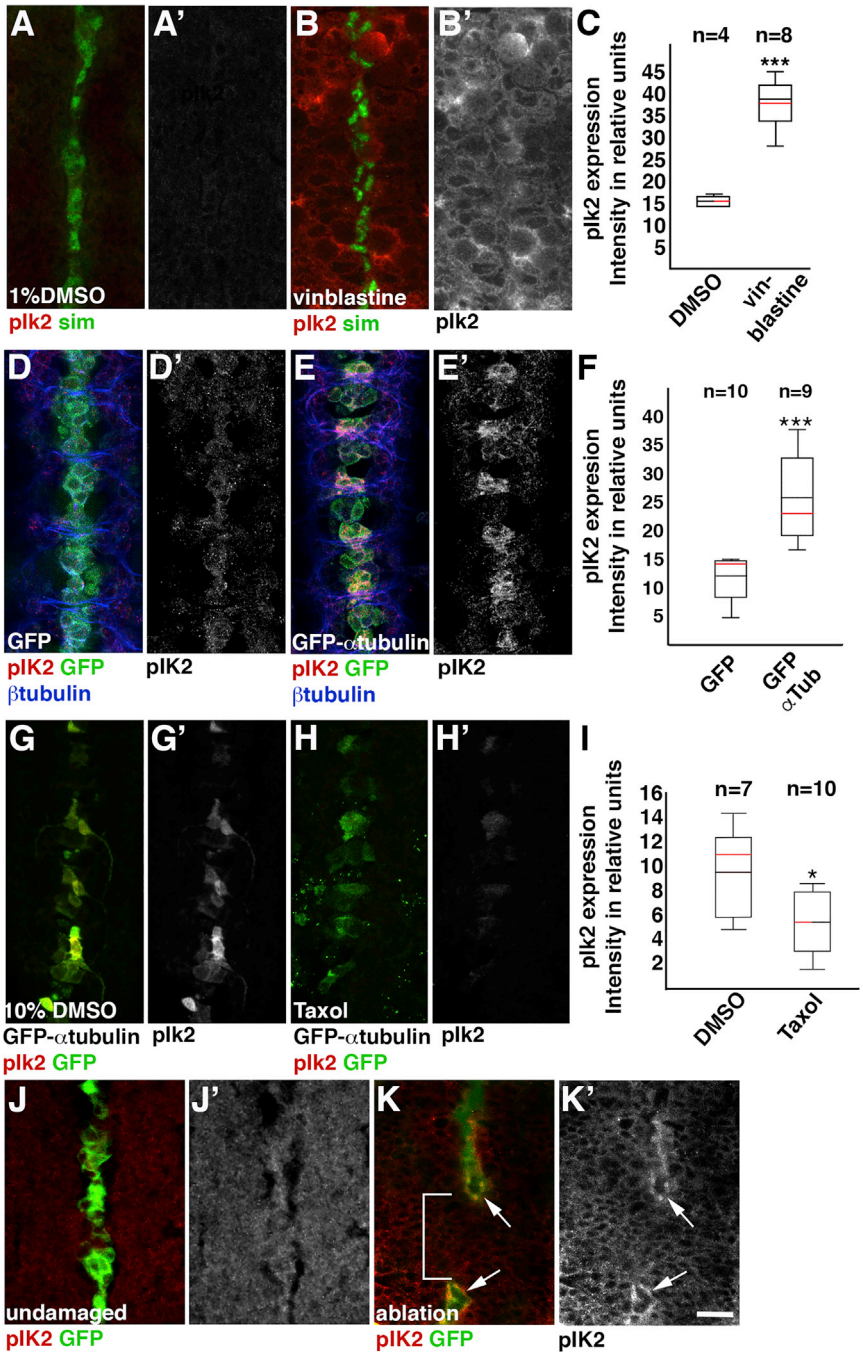

Figure 3. Microtubule disruption activates Ik2 phosphorylation (pIk2)

(A–C) Vinblastine injections depolymerize microtubules and trigger pIk2 (red) in the midline (green) and ventral ectoderm. Control vehicle injections are 1% DMSO (A). Embryos were fixed 10 min after injection. (A′) and (B′) show pIk2 only. (C) Quantification of pIk2 expression in DMSO- and vinblastine-injected WT embryos. Intensity, integrated density over a random area of 10,000 pixels. Wilcoxon rank-sum test. ***$p < 0.001$. Black line, average; red line, median. n, number of biological replicas (embryos). DMSO, x = 13; Vinblastine, x = 37.2.

(D–F) Expression of GFP-α-tubulin (green) at the midline leads to strong pIk2 expression (E, red). (D′) and (E′) show pIk2 only. (F) Quantification of pIk2 expression in *simG4>myrGFP* (GFP) and *simG4>GFP-α-tubulin62E* (GFPαTub) embryos. Intensity, integrated density of all midline cells. Wilcoxon rank-sum test. ***$p < 0.001$. Black line, average; red line, median. n, number of biological replicas (embryos). GFP, x = 12; GFP-α-Tub, x = 25.9

(G–I) In vehicle-injected embryos (10% DMSO), GFP-α-tubulin expression (green) results in strong pIk2 in midline cells (n = 10). (G′) shows pIk2 only. Taxol injections (1 mM) stabilize microtubules in midline GFP-α-tubulin-expressing embryos and reduce pIk2 expression. (H′) shows pIk2 only. (I) Quantification of pIk2 expression in DMSO- and Taxol-injected GFP-α-tubulin-expressing embryos. Intensity, integrated density of all midline cells. Wilcoxon rank-sum test. *$p < 0.05$. Black line, average; red line, median. n, number of biological replicas (embryos). DMSO, x = 9.6; Taxol, x = 5.5.

(J and K) Removal of cells at the midline (bracket) initiates pIk2 (red) proximal (arrows), but not distal to the tissue damage. (J) shows embryo without ablation. (J′) and (K′) show pIk2 only.

Genotypes are *wild-type* (A and B), *simG4>GFP-α-tubulin62E* (D, E, G, and H), and *simG4>myrGFP* (J and K). Embryonic stages are 11 (A, B, J, and K) and 13 (D, E, G, and H). Ventral views, anterior up. Scale bar, 10 μm.

the expression of Ik2DN, which reduces endogenous, damaged-induced, and vinblastine-induced midline divisions, increases the number of mitotic midline cells even further when expressed concurrently with α-tubulin (Figures 4M and 4N). Extra midline divisions caused by α-tubulin expression coincide with a strong phosphorylation of both endogenous Ik2 (Figures 4O–4P′ and 4R) and endogenous Tak1 (Figures 4S–4T′, and 4W). pIk2 (Figures 4Q and 4R) and Tak1 phosphorylation (Figures 4V and 4W) are enhanced by the co-expression of α-tubulin and Ik2DN. Compared to α-tubulin expression alone, co-expression with Ik2 does slightly increase Tak1 activation (Figures 4U and 4W). Finally, we detect a difference in the localization of the subcellular localization of GFP-α-tubulin when co-expressed with the two different Ik2 isoforms (Figures 4X–4Z). Simultaneous expression of GFP-α-tubulin with Ik2-myc results in an increased cortical accumulation of GFP-α-tubulin (Figure 4Y), but the co-expression of GFP-α-tubulin and Ik2DN increases cytoplasmic GFP-α-tubulin (Figure 4Z).

Our findings indicate that Ik2 has the ability to modulate both endogenous and ectopic midline divisions. The importance of the microtubule cytoskeleton is emphasized by the expression of α-tubulin together with Ik2 isoforms. This co-expression changes the properties of the Ik2 isoforms, turning the full length Ik2 into a mitotic suppressor, and Ik2DN into an activator.

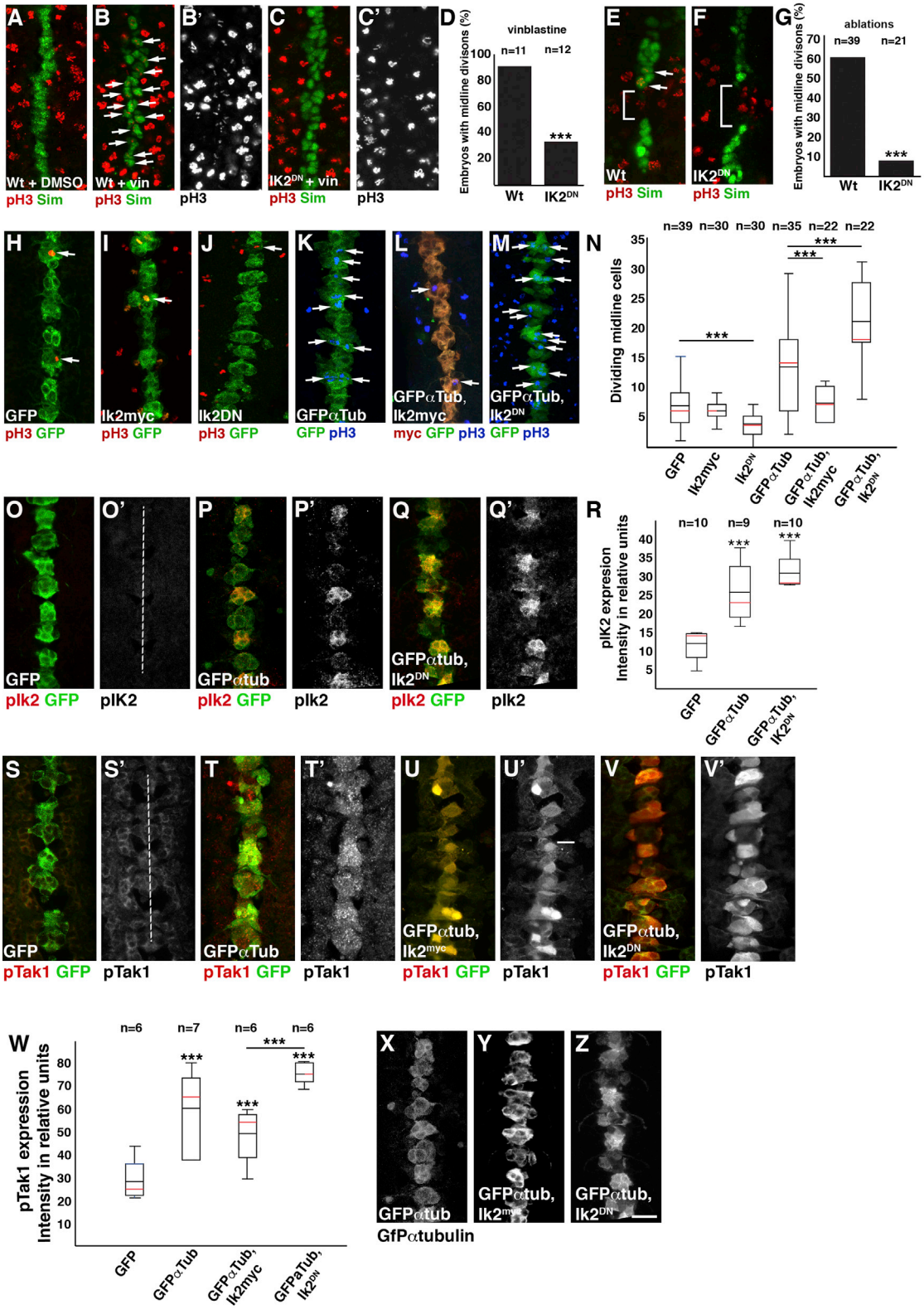

(legend on next page)

Expression of human Tau isoforms stimulate mitosis and TNF signaling at the ventral midline

Our experiments indicate that microtubule disruption causes midline cells to activate the TNF signaling cascade and enter into division. Accumulation of the microtubule binding protein Tau is crucial in the etiology of AD (Kumar et al., 2015). In human AD and mouse brains and in cell culture, the disruption of microtubules by hyperphosphorylated Tau has been reported (Ahlijanian et al., 2000; Alonso et al., 1997; Iqbal and Grundke-Iqbal, 2006; Sankaranarayanan et al., 2015). In *Drosophila* the ectopic expression of human Tau has been shown to cause hyperphosphorylation of the human Tau, but not the endogenous *Drosophila* Tau, and also to disrupt microtubules (Cowan et al., 2010; Sealey et al., 2017). We tested whether the expression of human Tau isoforms in midline cells can activate mitosis and TNF signaling. The expression of human 3-repeat Tau (3RTau), and to a lesser extent human 4-repeat Tau (4RTau), significantly increases mitotic activity at the midline (Figures 5A–5D). Expression of 3RTau (Khurana et al., 2006) also activates the phosphorylation of endogenous Tak1 (Figures 5E–5G), the expression and nuclear localization of Dorsal (Figures 5H–5J), and Jra expression (Figures 5K–5M).

In summary, ectopic expression of human Tau isoforms stimulates midline cell division and TNF signaling components, similar to GFP-α-tubulin expression or midline injury.

Activation of TNF signaling components is observed in AD brains concomitant with abnormal mitotic entry and cell death

We tested whether TNF signaling components and mitosis may also be activated in AD brains, where hyperphosphorylated Tau has been shown to disrupt microtubules (Alonso et al., 1997; Cowan et al., 2010). We used antibodies against phosphorylated Tak1, p65 (the closest ortholog to *Drosophila* Dorsal, DiOPT 9/15, http://flybase.org), phosphorylated Tbk1 (pTbk1; the closest ortholog to *Drosophila* Ik2, DiOPT 13/16, http://flybase.org), and diseased Tau (GT-38) (Gibbons et al., 2018). We focused on the subiculum area of the brain, the most inferior component to the hippocampal formation, where abnormal mitosis in AD brains has been previously reported (Busser et al., 1998; Nagy et al., 1997; Nakamura et al., 2020; Ogawa et al., 2003; Smith et al., 1999). We detect that phosphorylation of Tak1 is present in AD brains but almost absent from age-matched controls. Furthermore, Tak1 activation strongly colocalizes with diseased Tau (Figures 6A–6C). In addition, we also observed that p65 expression is nearly absent from controls but highly expressed in AD brains, and strongly colocalizes with diseased Tau (Figures 6D–6F). Inflammation is a hallmark in AD (Ortí-Casañ et al., 2019). The increased activation of TNF signaling in AD brains may be due to increased TNF signaling in non-neuronal cells, including glia and/or microglia that drive inflammatory responses in the brain. To distinguish between non-neuronal and neuronal cells, we examined the co-expression of pTak1 with the pan-neuronal marker NeuN (Figures 6G–6I). In control brains, pTak1 expression is rare, but 92% of the cells positive for pTak1 are neurons. In AD brains, pTak1 expression increases significantly (6.6 times), but now only 66% of pTak1 positive cells are neurons. This indicates that increased TNF signaling is not only observed in neurons but also significant in non-neuronal cells in AD brains. If pTak1 is activating Tbk1, then one would expect a near-complete absence of pTbk1 in controls and increased neuronal pTbk1 expression in

Figure 4. Ik2 is essential for mitotic activation at the midline after injury and in mid-embryogenesis

(A–C) Injection of the microtubule depolymerizer vinblastin (B) but not DMSO (A) in wild-type embryos triggers divisions (arrows, red, pH3) at the midline (green, Single Minded, Sim). Midline expression of dominant-negative Ik2 ($Ik2^{DN}$; C) suppresses vinblastine-activated midline divisions. Embryos were fixed 30–45 min after injection. (B′) and (C′) divisions only.

(D) Quantification of vinblastine injections. n, number of biological replicas (embryos). Fisher exact test, ***p < 0,001. Genotypes and scored numbers are Wt, *wild-type*, 10/11 embryos with divisions; $Ik2^{DN}$, *simG4>Ik2DN*, 4/12 embryos with divisions.

(E and F) Midline damage in wt embryos (E) triggers divisions around the damage site (arrows, red, pH3). Damage-induced divisions can be abolished by midline $Ik2^{DN}$ expression (F).

(G) Quantification of damage-induced divisions. n, number of biological replicas (embryos). Fisher exact test, ***p < 0.001. Genotypes and numbers are wt, *wild-type*, 29/36 embryos with divisions; *simG4>Ik2DN*, 2/21 embryos with divisions.

(H–J) Number of midline (green) divisions (red) are not affected by midline expression of myrGFP (H) or myc-tagged Ik2 (Ik2myc; I), but decrease with $Ik2^{DN}$ expression (J).

(K–M) Expression of GFP-α-tubulin (green, K) increases midline (green) cell divisions (blue). This increase can be suppressed by the simultaneous expression of Ik2myc (L, red) and is exacerbated by Ik2DN (M) expression.

(N) Quantification of modulation of midline cell division. Wilcoxon rank-sum test. ***p < 0.001, black line, median; red line, average. n, numbers of biological replicas (embryos). Genotypes and averages are GFP, *simG4>myrGFP*, x = 6.82; Ik2myc, *simG4>Ik2myc*, x = 6; $Ik2^{DN}$, simG4>$Ik2^{DN}$, x = 3.9, GFP-α-Tub, *simG4>GFP-α-tubulin62E*, x = 13.8; GFP-α-Tub, Ik2myc, *simG4>GFP-α-Tub; Ik2myc*, x = 7.7; GFP-α-Tub, $Ik2^{DN}$, *simG4>*$Ik2^{DN}$*; GFP-α-Tub*, x = 20.6.

(O–Q′) In midline GFP (green)-expressing embryos, pIK2 (red) is barely detectable (O). The midline expression of GFP-α-tubulin (green) activates Ik2 (P, red). This activation can be enhanced by the simultaneous expression of $Ik2^{DN}$ (Q) expression (stage 13). (O′), (P′), and (Q′) show pIk2 only. Dashed line marks midline.

(R) Quantification of pIk2 expression. Intensity, integrated density in relative units. Wilcoxon rank-sum test. ***p < 0.001, black line, median; red line, average. N, numbers of biological replicas (embryos). Genotypes and numbers are GFP, *simG4>myrGFP*, x = 12, *GFP-α-Tub, simG4>GFP-α-tubulin62E*, x = 25.9, GFP-α-Tub, $Ik2^{DN}$, *simG4>Ik2DN; GFP-α-Tub*, x = 30.8.

(S–V) Midline GFP-expressing embryos show Tak1 activation barely above background (S). Midline expression of GFP-α-tubulin (T) alone and in combination with Ik2myc (U) or $Ik2^{DN}$ (V) strongly activates Tak1. (S′), (T′), (U′), and (V′) show pTak1 only. Dashed line marks midline.

(W) Quantification of Tak1 activation. Intensity, integrated density in relative units. Wilcoxon rank-sum test. ***p < 0.001, black line, median; red line, average. n, number of biological replicas (embryos). Genotypes and numbers are GFP, *simG4>myrGFP*, x = 28.3, GFP-α-Tub, *simG4>GFP-α-tubulin62E*, x = 60.5, GFP-α-Tub, Ik2myc, *simG4>Ik2myc; GFP-α-Tub*, x = 49.5, GFP-α-Tub,$Ik2^{DN}$, *simG4>Ik2DN; GFP-α-Tub*, x = 75.9.

(X–Z) Midline expression of GFP-α-tubulin alone results in a cortical/cytoplasmic accumulation of the surplus tubulin (X). In contrast, GFP-α-tubulin expression combined with Ik2myc (Y) increases tubulin cortical localization, whereas combined with $Ik2^{DN}$, surplus tubulin is mainly cytoplasmic (Z). Embronic stages are stage 11 (A–C, E, and F) and stage 13 (H–Z). Ventral views, anterior up. Scale bar, 10 μm.

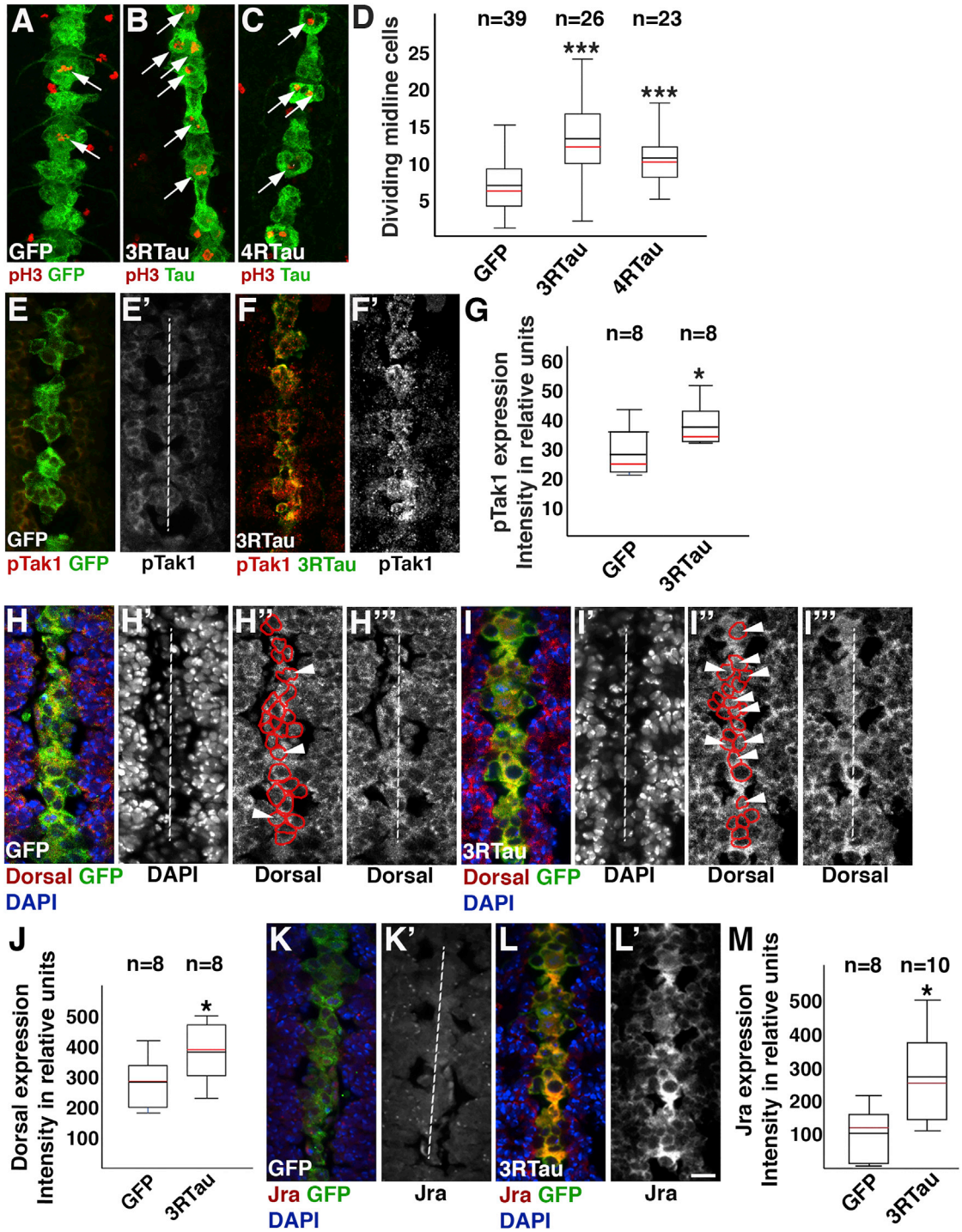

Figure 5. Human Tau expression activates mitosis, phosphorylation of Tak1, and expression of Dorsal and Jra/Jun

(A–C) Number of midline (green) cell divisions (red, arrows) increases upon expression of 3-repeat Tau (3RTau, B) and 4-repeat Tau (4RTau, C).

(D) Quantification of midline cell divisions upon human Tau expression. Student's t test, ***$p < 0.001$. Black line, average; red line, median. n, number of biological replicas (embryos). Genotypes and averages are GFP, *simG4>myrGFP*, x = 6.82; 3R Tau, *simG4>0n3Rtau*, x = 13; 4RTau, *simGal4>0n4Rtau/TM3*, x = 10.5.

(E and F) In GFP (green)-expressing midline cells, phosphorylation of Tak1 (red) is barely detectable (E). 3RTau expression significantly increases pTak1 expression (F). (E′) and (F′) show pTak1 only. Dashed line marks midline.

(G) Quantification of pTak1 expression. Student's t test *$p < 0.05$. Black line, average; red line, median. n, number of biological replicas (embryos). Genotypes and averages are GFP, *simG4>myrGFP*, x = 28.3; 3R Tau, *simG4>0n3Rtau*, x = 37.8.

(legend continued on next page)

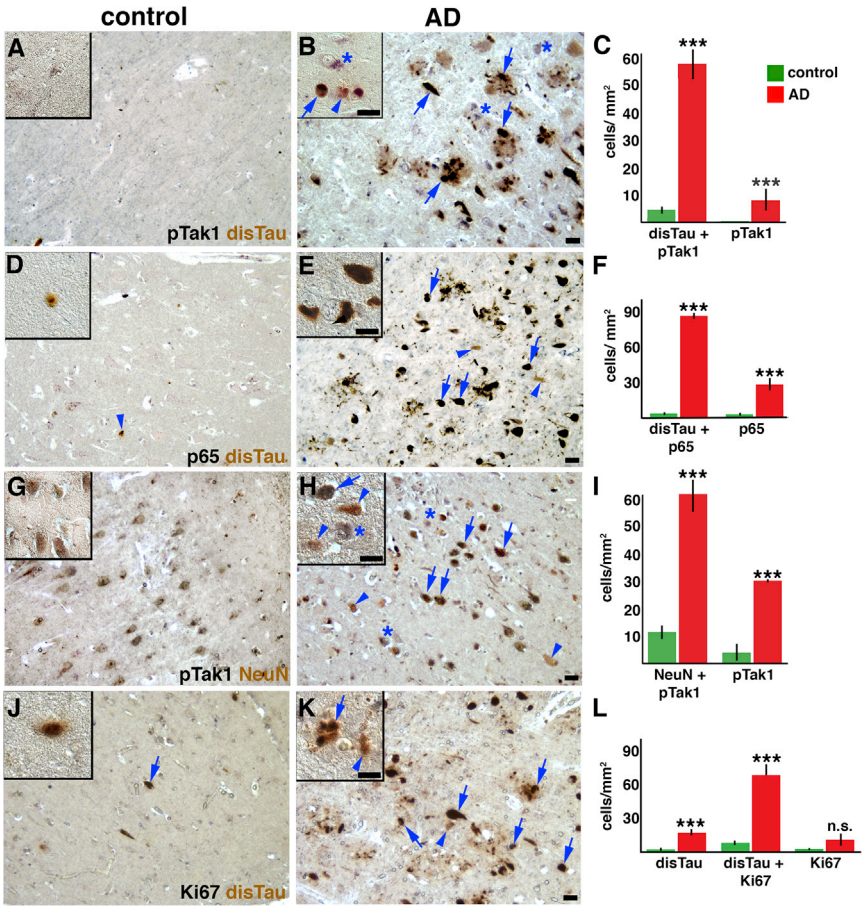

Figure 6. Activated Tak1, p65, and Ki67 are increased in AD brains

Subiculum region of human postmortem brains. Scale bar, 20 μm.

(A–C) Phosphorylation of Tak1 (seen in blue, asterisk, B) is rare in control brains and always co-localizes with diseased Tau (black, x = 4 cells/mm^2, A). (B) In AD brains, a minority of cells express only diseased Tau (brown, arrowhead, disTau) or only pTak1 (blue, asterisk, x = 9.2 cells/mm^2). Most cells are double stained (black, arrow, x = 57.7 cells/mm^2). Insets show higher magnification of a second sample. (C) Quantification of pTak1 expression and diseased Tau in control (green columns) and AD brains (red columns); bars represent SEMs. ***p < 0.001 Mann-Whitney *U* test, n = 3 brain slices from 3 patients for control and AD.

(D–F) p65 (blue), the ortholog of *Drosophila* Dorsal, is barely detectable in age-matched control brains (x = 6.17 cells/mm^2; 3.37 cells/mm^2 colocalized with diseased Tau). However, in AD brains, most cells (x = 85.9 cells/mm^2) are double stained (black, arrow), with a minority (x = 31.3 cells/mm^2) being only diseased Tau$^+$ (brown, arrowhead). Insets at top left show higher magnification of a second sample. (F) Quantification of p65 expression and diseased Tau in control (green columns) and AD brains (red columns); bars represent SEMs. ***p < 0.0001, Mann-Whitney *U* test, n = 3 brain slices from 3 patients for control and AD.

(G–I) Activation of Tak1 is mainly neuronal.

(G) In subiculums of control brains, phosphorylation of Tak1 is rare, but if present, it is mainly detectable in neurons (91%, 13.26 cells/mm^2 of 14.49 cells/mm^2).

(H) AD brains exhibit a drastic increase in pTak1 expression in neurons (66%, x = 61.8 cells/mm^2) as well as non-neuronal cells (34%, x = 31.8 cells/mm^2).

(I) Quantification of pTak1 expression and NeuN in control (green columns) and AD brains (red columns); bars represent SEMs. ***p < 0.0001, Mann-Whitney *U* test, n = 3 brain slices from 3 patients for control and AD. Asterisk labels pTak1 only (blue). Arrowheads label NeuN only (brown). Arrows label pTak1/NeuN double stained cells (black)

(J–L) Dividing cells (blue, x = 1.98 cells/mm^2) or cells expressing diseased Tau (brown, arrowhead, x = 2.41 cells/mm^2) are nearly absent from the subiculum of control brains (J), but when present, they often colocalize with diseased Tau (arrow, x = 7.9 cells/mm^2).

(K) In AD brains, the number of dividing cells increases (x = 85.3 cells/mm^2). Most dividing cells colocalize with diseased Tau (arrow, x = 73.46 cells/mm^2).

AD brains. We detect a dramatic (14 times) increase in the phosphorylation of Tbk1 in neurons, corresponding to 92% of all pTbk1 cells in AD brains (Figures S2A–S2C). Both pTak1$^+$ and pTbk1$^+$ cells appear distributed randomly throughout the subiculum region. Interestingly, three times more neurons express pTak1 than pTbk1 (compare Figures 6L and S2C). The proportion of pTbk1$^+$ neurons of total pTbk1 cells remains similar between control (93%) and AD brains (91%), suggesting that Tbk1 activation is predominantly neuron specific.

The colocalization of diseased Tau with pTak1 and p65 expression levels suggests that microtubule disruption in AD brains may activate a similar pathway, as we discovered for damage-induced mitosis in *Drosophila* midline cells. Interestingly, we detect an increase (8 times) in proliferating cells in AD brains, with 86% of cells double positive for cell-cycle marker Ki67 and diseased Tau (Figures 6J–6L). Next, we analyzed the activation of Tbk1 expression in combination with Ki67. We again observed a significant increase in Ki67$^+$ cells, and 50% of all

(H and I) Compared to midline GFP-expressing controls (H), 3RTau expression (I) activates Dorsal in midline cells and Dorsal nuclear entry (arrowheads). Nuclei encircled red (H″ and I″). (H′) and (I′) show DAPI only. (H″), (H‴), (I″), and (I‴) show Dorsal only. Dashed line marks midline.

(J) Quantification of Dorsal expression. Student's t test *p < 0.05. Black line, average; red line, median. n, number of biological replicas (embryos). Genotypes and averages are GFP, *simG4>myrGFP*, x = 281.7; 3R Tau, *simG4>0n3Rtau*, x = 381.4.

(K and L) Jra is just detectable in GFP-expressing controls (K). 3RTau expression (L) increases Jra expression in midline cells. (K′) and (L′) show Jra only. Dashed line marks midline.

(M) Quantification of Jra expression. Student's t test *p < 0.05. Black line, average; red line, median. n, number of biological replicas (embryos). Genotypes and averages are GFP, *simG4>myrGFP*, x = 150.6; 3R Tau, *simG4>0n3Rtau*, x = 270.6. Ventral views, anterior up. Scale bar, 20 μm.

pTbk1 cells show colocalization with Ki67 (Figures S2D–S2F). Ectopic activation of the cell cycle in mature neurons is thought to activate apoptosis (Herrup, 2012). In accordance, 81% of pTbk1^{+} cells are positive for the apoptotic marker cleaved caspase-3 (Figures S2G–S2I). Finally, we noted a significant overlap (75%) between pTbk1 and cleaved caspase-3 in controls, indicating that the activation of pTbk1 correlates strongly with cell death. However, 50% of all cleaved caspase-3^{+} cells do not show colocalization with pTbk1 expression.

In summary, the activation of TNF signaling components Tak1, Tbk1, and p65 (NFkappaB) in AD brains, and the observed expression colocalizations with abnormal Tau, suggest that microtubule disruption in human brains may activate a similar signaling pathway, as we discovered using the *Drosophila* midline model.

DISCUSSION

We have previously reported that mitotic activation in midline cells can be triggered by microtubule disruption. In contrast, microtubule stabilization, actin depolymerization, loss of cadherin adhesion, or loss of cell polarity are unable to induce cell divisions in midline cells (Bossing et al., 2012). Here, we show that traumatic, chemical, or genetic disruption of microtubules in midline cells triggers phosphorylation of the TNF signaling kinases Tak1 and Ik2, which activate Dorsal expression and translocation into nuclei and are required for entry into division.

Previous studies have linked external TNF signaling activity and microtubule stability (Chopra et al., 2014; Jackman et al., 2009; Petrache et al., 2003). Since Egr/TNF in *Drosophila* is expressed in segmentally repeated stripes, cell ablation and chemical depolymerization of microtubules may result in changes in the environment, bringing cells closer to or disrupting TNF sources (Figure S1), thereby changing external TNF signaling and subsequently affecting microtubules. Our results, however, demonstrate for the first time that phosphorylation of Tak1 and Ik2 and nuclear entry of Dorsal can be initiated from inside cells by the targeted expression of α-tubulin or of human Tau isoforms, which do not visibly interfere with cell shape or location. How can changes to the microtubules inside cells trigger TNF signaling components? Both kinases Ik2 and Tak1 have close links with microtubules. In *Drosophila*, Ik2 binds microtubules via Spn-F (Otani et al., 2011), and targeted expression of Ik2 has been shown to increase cell death and microtubule breakage in sensory neurons (Lee et al., 2009). In proteomic analysis of *Drosophila* immunity responses, α-tubulin has been identified as a predominant binding partner of Tak1 (Fukuyama et al., 2013). In addition, in the mouse brain, Tak1 stabilizes microtubules via α-Tat1, thereby permitting microtubules to sequester Akt and decreasing Akt, glycogen synthase kinase 3β (GSK3β), and c-*myc* signaling (Shah et al., 2018). We show that midline-targeted Ik2 tightly colocalizes with microtubules (Figure 4L) and that Ik2 may contribute to microtubule stability (Figures 4X–4Z). Co-expression of GFP-α-tubulin and Ik2 results in a strong accumulation of GFP-α-tubulin in the cytoplasm and along the cell cortex, but not in nuclei. This co-expression also reduces midline division numbers to levels similar to those seen in wild type (Figure 4N). In contrast, co-expression of GFP-α-tubulin and a non-phosphorylatable form of Ik2 (Ik2DN) decreases GFP-α-tubulin along the cortex but increases diffuse localization in cytoplasm and nuclei, suggesting reduced polymerization. In addition, Ik2DN/GFP-α-tubulin co-expression leads to increased phosphorylation of endogenous Tak1 and Ik2, resulting in increased cell division (Figure 4O). Finally, the activation of Ik2 by midline targeted α-tubulin can be reduced by the stabilization of microtubules with Taxol injections. Our findings indicate that stable microtubules inactivate pIk2, whereas microtubule disruption results in Ik2 activation and subsequent mitotic entry. In addition, the extent of microtubule polymerization also interferes with Tak1 activation, which is in turn needed to activate Ik2. Tak1 dimerization is sufficient for its activation (Kishimoto et al., 2000), and as shown for Akt signaling, intact microtubules may prevent Tak1 dimerization by sequestration (Shah et al., 2018).

The final outcome of TNF signal activation is the nuclear translocation of Dorsal/NfkappaB (p65). Our experiments confirm that microtubule disruption triggers the expression and nuclear entry of Dorsal. Dorsal expression in midline cells activates Jun, but not Fos, and Jun expression is essential for damaged induced midline divisions (Bossing et al., 2012). During regeneration of the *Drosophila* intestine and imaginal discs (Martín and Morata, 2018; Panayidou and Apidianakis, 2013) and in the mammalian liver (Stepniak et al., 2006), the activation of Jun kinase signaling results in the formation of Jun/ Fos heterodimers creating the AP-1 transcription factor that is pivotal for cell survival (Bejjani et al., 2019). The absence of Fos expression in the midline excludes the formation of AP-1. In addition, using the midline model, we show that the activation of the Jun kinase pathway is able to suppress the Dorsal-driven mitosis. Thus, the activation of mitosis after midline damage seems to be independent from either AP-1 transcription or Jun kinase signaling.

Tak1, Ik2, and microtubules are widely conserved, which prompted us to test whether microtubule disruption and mitotic activation may be linked in other systems. The accumulation of hyperphosphorylated Tau proteins in AD brains results in microtubule damage (Alonso et al., 1997; Cowan et al., 2010). We found that the expression of human Tau isoforms, which have previously been shown to become hyperphosphorylated (Cowan et al., 2010; Sealey et al., 2017), activates midline cell division in the *Drosophila* embryonic CNS. Crucially, we demonstrate that human Tau also drives the phosphorylation of endogenous *Drosophila* Tak1, Dorsal expression and its nuclear entry, and Jra expression. These are the same components activated by microtubule damage following α-tubulin expression. Next, we tested for the activation of Tak1 and the ortholog of *Drosophila* Ik2, Tbk1, in postmortem AD brains. We focused on the subiculum of the hippocampal formation since it is a region where abnormal cycling cells have been observed (Busser et al., 1998; Nagy et al., 1997; Nakamura et al., 2020; Ogawa et al., 2003; Smith et al., 1999). We readily detected the activation of Tak1 and Tbk1 in AD brains but only rarely in controls. Both kinases are mainly expressed in mature neurons and the activation of Tak1, and p65, the ortholog of *Drosophila* Dorsal, colocalizes tightly with diseased Tau, opening up the possibility that a link between microtubule disruption and Tak1 activation may also exist in this context.

In various neurodegenerative diseases, mitotic activation in mature neurons has been repeatedly reported and is thought to trigger apoptosis (Busser et al., 1998; Copani et al., 1999,

2001; Frade and Ovejero-Benito, 2015; Herrup, 2012; Hisanaga and Endo, 2010; Husseman et al., 2000; Marlier et al., 2020; Park et al., 2007; Tian et al., 2009). In AD, abnormal neuronal entry into mitosis (Arendt, 2012; Bonda et al., 2009; Mosch et al., 2007; Pei et al., 2002) is reported to result in an arrest in G1/S phase and a mitotic catastrophe (Ogawa et al., 2003; Tweedie et al., 2007). Tbk1 has roles in cell division (Pillai et al., 2015) and neurodegenerative diseases (Freischmidt et al., 2015; van der Zee et al., 2017). We observed that pTbk1 and the mitotic Ki67 marker partially colocalize in the AD subiculum, with the latter also co-localizing with diseased Tau. In addition, increased Tbk1 phosphorylation strongly overlaps with the cell death indicator-activated caspase 3. Although nearly all pTbk1^{+} cells co-express activated caspase 3, the majority of caspase 3 cells do not express activated Tbk1. The discrepancy between the frequency of mitotic activation and cell death may indicate that Tbk1 phosphorylation triggers apoptosis not exclusively via mitotic activation. It may also be possible that pTbk1 activates abnormal cell-cycle entry, but, as previously reported in AD brains, neurons fail to complete and arrest in mitosis (Ogawa et al., 2003; Tweedie et al., 2007), and pTbk is eventually dephosphorylated.

The limitation in sample numbers and examined human brain regions do not allow us to postulate a direct link between Tbk1 and Tak1 activation in neurons, abnormal mitosis, and cell death, but our results suggest a potential connection. Additional studies using, for example, induced pluripotent stem cell-derived neurons from healthy and AD patients, are required to confirm the underlying mechanism.

Our findings support the role of microtubules as a crucial cell-signaling regulator. We demonstrate that microtubule disruption from inside cells can activate Tak1 and Ik2/Tbk1 kinases of the TNF pathway, thereby triggering mitotic entry and damage repair in *Drosophila* midline CNS cells. Activation of TNF signaling has been implicated in repair after injuries to glia cells (Kato et al., 2018). It will be important to determine whether it also may play a role in the etiology of neurodegenerative diseases.

STAR★METHODS

Detailed methods are provided in the online version of this paper and include the following:

- KEY RESOURCES TABLE
- RESOURCE AVAILABILITY
  - Lead contact
  - Materials availability
  - Data and code availability
- EXPERIMENTAL MODEL AND SUBJECT DETAILS
  - Fly stocks
  - Human post-mortem brain tissue
- METHOD DETAILS
  - Cell ablation and embryo injections
  - Immunohistochemistry
  - Generation of MyD88 and MyD88DN transgenics
  - Immunohistochemistry of human brain tissue and image analysis
- QUANTIFICATION AND STATISTICAL ANALYSIS

SUPPLEMENTAL INFORMATION

Supplemental information can be found online at https://doi.org/10.1016/j.celrep.2021.109325.

ACKNOWLEDGMENTS

We would like to thank the South West Dementia Brain Bank (SWDBB) for providing brain tissue for this study. For the supply of antisera, we are grateful to S.A. Wasserman, S. Hiyashi, S. Crews, and the Developmental Studies Hybridoma Bank (DSHB) at the University of Iowa. The project was funded by the School of Biomedical Sciences (T.B.) and the Peninsula Medical School (T.B. and C.B.), University of Plymouth, U.K.

AUTHOR CONTRIBUTIONS

Conceptualization, T.B. Experiments performed and analyzed, T.B. and C.S.B. Manuscript written and revised, T.B. and C.S.B.

DECLARATION OF INTERESTS

The authors declare no competing interests.

Received: September 9, 2019
Revised: November 12, 2020
Accepted: June 8, 2021
Published: July 6, 2021

REFERENCES

Ahlijanian, M.K., Barrezueta, N.X., Williams, R.D., Jakowski, A., Kowsz, K.P., McCarthy, S., Coskran, T., Carlo, A., Seymour, P.A., Burkhardt, J.E., et al. (2000). Hyperphosphorylated tau and neurofilament and cytoskeletal disruptions in mice overexpressing human p25, an activator of cdk5. Proc. Natl. Acad. Sci. USA *97*, 2910–2915.

Alonso, A.D., Grundke-Iqbal, I., Barra, H.S., and Iqbal, K. (1997). Abnormal phosphorylation of tau and the mechanism of Alzheimer neurofibrillary degeneration: sequestration of microtubule-associated proteins 1 and 2 and the disassembly of microtubules by the abnormal tau. Proc. Natl. Acad. Sci. USA *94*, 298–303.

Arendt, T. (2012). Cell cycle activation and aneuploid neurons in Alzheimer's disease. Mol. Neurobiol. *46*, 125–135.

Bejjani, F., Evanno, E., Zibara, K., Piechaczyk, M., and Jariel-Encontre, I. (2019). The AP-1 transcriptional complex: local switch or remote command? Biochim. Biophys. Acta Rev. Cancer *1872*, 11–23.

Bely, A.E., and Nyberg, K.G. (2010). Evolution of animal regeneration: re-emergence of a field. Trends Ecol. Evol. *25*, 161–170.

Blonska, M., Shambharkar, P.B., Kobayashi, M., Zhang, D., Sakurai, H., Su, B., and Lin, X. (2005). TAK1 is recruited to the tumor necrosis factor-alpha (TNF-alpha) receptor 1 complex in a receptor-interacting protein (RIP)-dependent manner and cooperates with MEKK3 leading to NF-kappaB activation. J. Biol. Chem. *280*, 43056–43063.

Bonda, D.J., Evans, T.A., Santocanale, C., Llosá, J.C., Viña, J., Bajic, V., Castellani, R.J., Siedlak, S.L., Perry, G., Smith, M.A., and Lee, H.G. (2009). Evidence for the progression through S-phase in the ectopic cell cycle re-entry of neurons in Alzheimer disease. Aging (Albany NY) *1*, 382–388.

Bossing, T., and Brand, A.H. (2006). Determination of cell fate along the anteroposterior axis of the Drosophila ventral midline. Development *133*, 1001–1012.

Bossing, T., and Technau, G.M. (1994). The fate of the CNS midline progenitors in Drosophila as revealed by a new method for single cell labelling. Development *120*, 1895–1906.

Bossing, T., Barros, C.S., Fischer, B., Russell, S., and Shepherd, D. (2012). Disruption of microtubule integrity initiates mitosis during CNS repair. Dev. Cell *23*, 433–440.

Busser, J., Geldmacher, D.S., and Herrup, K. (1998). Ectopic cell cycle proteins predict the sites of neuronal cell death in Alzheimer's disease brain. J. Neurosci. *18*, 2801–2807.

Chang, E.H., Adorjan, I., Mundim, M.V., Sun, B., Dizon, M.L., and Szele, F.G. (2016). Traumatic Brain Injury Activation of the Adult Subventricular Zone Neurogenic Niche. Front. Neurosci. *10*, 332.

Chopra, A., Anderson, A., and Giardina, C. (2014). Novel piperazine-based compounds inhibit microtubule dynamics and sensitize colon cancer cells to tumor necrosis factor-induced apoptosis. J. Biol. Chem. *289*, 2978–2991.

Copani, A., Condorelli, F., Caruso, A., Vancheri, C., Sala, A., Giuffrida Stella, A.M., Canonico, P.L., Nicoletti, F., and Sortino, M.A. (1999). Mitotic signaling by beta-amyloid causes neuronal death. FASEB J. *13*, 2225–2234.

Copani, A., Uberti, D., Sortino, M.A., Bruno, V., Nicoletti, F., and Memo, M. (2001). Activation of cell-cycle-associated proteins in neuronal death: a mandatory or dispensable path? Trends Neurosci. *24*, 25–31.

Cowan, C.M., Bossing, T., Page, A., Shepherd, D., and Mudher, A. (2010). Soluble hyper-phosphorylated tau causes microtubule breakdown and functionally compromises normal tau in vivo. Acta Neuropathol. *120*, 593–604.

Evans, T., Kok, W.L., Cowan, K., Hefford, M., and Anichtchik, O. (2018). Accumulation of beta-synuclein in cortical neurons is associated with autophagy attenuation in the brains of dementia with Lewy body patients. Brain Res. *1681*, 1–13.

Forbes, S.J., and Rosenthal, N. (2014). Preparing the ground for tissue regeneration: from mechanism to therapy. Nat. Med. *20*, 857–869.

Frade, J.M., and Ovejero-Benito, M.C. (2015). Neuronal cell cycle: the neuron itself and its circumstances. Cell Cycle *14*, 712–720.

Freischmidt, A., Wieland, T., Richter, B., Ruf, W., Schaeffer, V., Müller, K., Marroquin, N., Nordin, F., Hübers, A., Weydt, P., et al. (2015). Haploinsufficiency of TBK1 causes familial ALS and fronto-temporal dementia. Nat. Neurosci. *18*, 631–636.

Fukuyama, H., Verdier, Y., Guan, Y., Makino-Okamura, C., Shilova, V., Liu, X., Maksoud, E., Matsubayashi, J., Haddad, I., Spirohn, K., et al. (2013). Landscape of protein-protein interactions in Drosophila immune deficiency signaling during bacterial challenge. Proc. Natl. Acad. Sci. USA *110*, 10717–10722.

Fulga, T.A., Elson-Schwab, I., Khurana, V., Steinhilb, M.L., Spires, T.L., Hyman, B.T., and Feany, M.B. (2007). Abnormal bundling and accumulation of F-actin mediates tau-induced neuronal degeneration in vivo. Nat. Cell Biol. *9*, 139–148.

Garcia-Reitböck, P., Anichtchik, O., Bellucci, A., Iovino, M., Ballini, C., Fineberg, E., Ghetti, B., Della Corte, L., Spano, P., Tofaris, G.K., et al. (2010). SNARE protein redistribution and synaptic failure in a transgenic mouse model of Parkinson's disease. Brain *133*, 2032–2044.

Gibbons, G.S., Banks, R.A., Kim, B., Changolkar, L., Riddle, D.M., Leight, S.N., Irwin, D.J., Trojanowski, J.Q., and Lee, V.M.Y. (2018). Detection of Alzheimer Disease (AD)-Specific Tau Pathology in AD and NonAD Tauopathies by Immunohistochemistry With Novel Conformation-Selective Tau Antibodies. J. Neuropathol. Exp. Neurol. *77*, 216–228.

Hayden, M.S., and Ghosh, S. (2004). Signaling to NF-kappaB. Genes Dev. *18*, 2195–2224.

Herrup, K. (2012). The contributions of unscheduled neuronal cell cycle events to the death of neurons in Alzheimer's disease. Front. Biosci. (Elite Ed.) *4*, 2101–2109.

Hisanaga, S., and Endo, R. (2010). Regulation and role of cyclin-dependent kinase activity in neuronal survival and death. J. Neurochem. *115*, 1309–1321.

Horng, T., and Medzhitov, R. (2001). Drosophila MyD88 is an adapter in the Toll signaling pathway. Proc. Natl. Acad. Sci. USA *98*, 12654–12658.

Hu, X., Yagi, Y., Tanji, T., Zhou, S., and Ip, Y.T. (2004). Multimerization and interaction of Toll and Spätzle in Drosophila. Proc. Natl. Acad. Sci. USA *101*, 9369–9374.

Huang, L., Ohsako, S., and Tanda, S. (2005). The lesswright mutation activates Rel-related proteins, leading to overproduction of larval hemocytes in Drosophila melanogaster. Dev. Biol. *280*, 407–420.

Husseman, J.W., Nochlin, D., and Vincent, I. (2000). Mitotic activation: a convergent mechanism for a cohort of neurodegenerative diseases. Neurobiol. Aging *21*, 815–828.

Iqbal, K., and Grundke-Iqbal, I. (2006). Discoveries of tau, abnormally hyperphosphorylated tau and others of neurofibrillary degeneration: a personal historical perspective. J. Alzheimers Dis. *9* (*3, Suppl*), 219–242.

Jackman, R.W., Rhoads, M.G., Cornwell, E., and Kandarian, S.C. (2009). Microtubule-mediated NF-kappaB activation in the TNF-alpha signaling pathway. Exp. Cell Res. *315*, 3242–3249.

Kato, K., Losada-Perez, M., and Hidalgo, A. (2018). Gene network underlying the glial regenerative response to central nervous system injury. Dev. Dyn. *247*, 85–93.

Kauppila, S., Maaty, W.S., Chen, P., Tomar, R.S., Eby, M.T., Chapo, J., Chew, S., Rathore, N., Zachariah, S., Sinha, S.K., et al. (2003). Eiger and its receptor, Wengen, comprise a TNF-like system in Drosophila. Oncogene *22*, 4860–4867.

Khurana, V., Lu, Y., Steinhilb, M.L., Oldham, S., Shulman, J.M., and Feany, M.B. (2006). TOR-mediated cell-cycle activation causes neurodegeneration in a Drosophila tauopathy model. Curr. Biol. *16*, 230–241.

Kishimoto, K., Matsumoto, K., and Ninomiya-Tsuji, J. (2000). TAK1 mitogen-activated protein kinase kinase kinase is activated by autophosphorylation within its activation loop. J. Biol. Chem. *275*, 7359–7364.

Klaes, A., Menne, T., Stollewerk, A., Scholz, H., and Klämbt, C. (1994). The Ets transcription factors encoded by the Drosophila gene pointed direct glial cell differentiation in the embryonic CNS. Cell *78*, 149–160.

Kumar, A., Singh, A., and Ekavali. (2015). A review on Alzheimer's disease pathophysiology and its management: an update. Pharmacol. Rep. *67*, 195–203.

Lee, H.H., Jan, L.Y., and Jan, Y.N. (2009). Drosophila IKK-related kinase Ik2 and Katanin p60-like 1 regulate dendrite pruning of sensory neuron during metamorphosis. Proc. Natl. Acad. Sci. USA *106*, 6363–6368.

Lin, T., Pan, P.Y., Lai, Y.T., Chiang, K.W., Hsieh, H.L., Wu, Y.P., Ke, J.M., Lee, M.C., Liao, S.S., Shih, H.T., et al. (2015). Spindle-F Is the Central Mediator of Ik2 Kinase-Dependent Dendrite Pruning in Drosophila Sensory Neurons. PLoS Genet. *11*, e1005642.

Marlier, Q., D'aes, T., Verteneuil, S., Vandenbosch, R., and Malgrange, B. (2020). Core cell cycle machinery is crucially involved in both life and death of post-mitotic neurons. Cell. Mol. Life Sci. *77*, 4553–4571.

Martín, R., and Morata, G. (2018). Regenerative response of different regions of Drosophila imaginal discs. Int. J. Dev. Biol. *62*, 507–512.

Mosch, B., Morawski, M., Mittag, A., Lenz, D., Tarnok, A., and Arendt, T. (2007). Aneuploidy and DNA replication in the normal human brain and Alzheimer's disease. J. Neurosci. *27*, 6859–6867.

Nagy, Z., Esiri, M.M., Cato, A.M., and Smith, A.D. (1997). Cell cycle markers in the hippocampus in Alzheimer's disease. Acta Neuropathol. *94*, 6–15.

Nakamura, M., Kaneko, S., Dickson, D.W., and Kusaka, H. (2020). Aberrant Accumulation of BRCA1 in Alzheimer Disease and Other Tauopathies. J. Neuropathol. Exp. Neurol. *79*, 22–33.

Ogawa, O., Zhu, X., Lee, H.G., Raina, A., Obrenovich, M.E., Bowser, R., Ghanbari, H.A., Castellani, R.J., Perry, G., and Smith, M.A. (2003). Ectopic localization of phosphorylated histone H3 in Alzheimer's disease: a mitotic catastrophe? Acta Neuropathol. *105*, 524–528.

Ortí-Casañ, N., Wu, Y., Naudé, P.J.W., De Deyn, P.P., Zuhorn, I.S., and Eisel, U.L.M. (2019). Targeting TNFR2 as a Novel Therapeutic Strategy for Alzheimer's Disease. Front. Neurosci. *13*, 49.

Oshima, K., Takeda, M., Kuranaga, E., Ueda, R., Aigaki, T., Miura, M., and Hayashi, S. (2006). IKK epsilon regulates F actin assembly and interacts with Drosophila IAP1 in cellular morphogenesis. Curr. Biol. *16*, 1531–1537.

Otani, T., Oshima, K., Onishi, S., Takeda, M., Shinmyozu, K., Yonemura, S., and Hayashi, S. (2011). IKKε regulates cell elongation through recycling endosome shuttling. Dev. Cell *20*, 219–232.

Panayidou, S., and Apidianakis, Y. (2013). Regenerative inflammation: lessons from Drosophila intestinal epithelium in health and disease. Pathogens *2*, 209–231.

Park, K.H., Hallows, J.L., Chakrabarty, P., Davies, P., and Vincent, I. (2007). Conditional neuronal simian virus 40 T antigen expression induces Alzheimer-like tau and amyloid pathology in mice. J. Neurosci. *27*, 2969–2978.

Pei, J.J., Braak, H., Gong, C.X., Grundke-Iqbal, I., Iqbal, K., Winblad, B., and Cowburn, R.F. (2002). Up-regulation of cell division cycle (cdc) 2 kinase in neurons with early stage Alzheimer's disease neurofibrillary degeneration. Acta Neuropathol. *104*, 369–376.

Petrache, I., Birukova, A., Ramirez, S.I., Garcia, J.G., and Verin, A.D. (2003). The role of the microtubules in tumor necrosis factor-alpha-induced endothelial cell permeability. Am. J. Respir. Cell Mol. Biol. *28*, 574–581.

Pillai, S., Nguyen, J., Johnson, J., Haura, E., Coppola, D., and Chellappan, S. (2015). Tank binding kinase 1 is a centrosome-associated kinase necessary for microtubule dynamics and mitosis. Nat. Commun. *6*, 10072.

Ricci, L., and Srivastava, M. (2018). Wound-induced cell proliferation during animal regeneration. Wiley Interdiscip. Rev. Dev. Biol. *7*, e321.

Robertson, H.M., Preston, C.R., Phillis, R.W., Johnson-Schlitz, D.M., Benz, W.K., and Engels, W.R. (1988). A stable genomic source of P element transposase in Drosophila melanogaster. Genetics *118*, 461–470.

Ruddy, R.M., and Morshead, C.M. (2018). Home sweet home: the neural stem cell niche throughout development and after injury. Cell Tissue Res. *371*, 125–141.

Sankaranarayanan, S., Barten, D.M., Vana, L., Devidze, N., Yang, L., Cadelina, G., Hoque, N., DeCarr, L., Keenan, S., Lin, A., et al. (2015). Passive immunization with phospho-tau antibodies reduces tau pathology and functional deficits in two distinct mouse tauopathy models. PLoS ONE *10*, e0125614.

Schmidt-Ott, U., and Technau, G.M. (1992). Expression of en and wg in the embryonic head and brain of Drosophila indicates a refolded band of seven segment remnants. Development *116*, 111–125.

Scholz, H., Sadlowski, E., Klaes, A., and Klämbt, C. (1997). Control of midline glia development in the embryonic Drosophila CNS. Mech. Dev. *62*, 79–91.

Sealey, M.A., Vourkou, E., Cowan, C.M., Bossing, T., Quraishe, S., Grammenoudi, S., Skoulakis, E.M.C., and Mudher, A. (2017). Distinct phenotypes of three-repeat and four-repeat human tau in a transgenic model of tauopathy. Neurobiol. Dis. *105*, 74–83.

Shah, N., Kumar, S., Zaman, N., Pan, C.C., Bloodworth, J.C., Lei, W., Streicher, J.M., Hempel, N., Mythreye, K., and Lee, N.Y. (2018). TAK1 activation of alpha-TAT1 and microtubule hyperacetylation control AKT signaling and cell growth. Nat. Commun. *9*, 1696.

Shen, B., Liu, H., Skolnik, E.Y., and Manley, J.L. (2001). Physical and functional interactions between Drosophila TRAF2 and Pelle kinase contribute to Dorsal activation. Proc. Natl. Acad. Sci. USA *98*, 8596–8601.

Smith, M.Z., Nagy, Z., and Esiri, M.M. (1999). Cell cycle-related protein expression in vascular dementia and Alzheimer's disease. Neurosci. Lett. *271*, 45–48.

Stepniak, E., Ricci, R., Eferl, R., Sumara, G., Sumara, I., Rath, M., Hui, L., and Wagner, E.F. (2006). c-Jun/AP-1 controls liver regeneration by repressing p53/p21 and p38 MAPK activity. Genes Dev. *20*, 2306–2314.

Tian, B., Yang, Q., and Mao, Z. (2009). Phosphorylation of ATM by Cdk5 mediates DNA damage signalling and regulates neuronal death. Nat. Cell Biol. *11*, 211–218.

Tweedie, D., Sambamurti, K., and Greig, N.H. (2007). TNF-alpha inhibition as a treatment strategy for neurodegenerative disorders: new drug candidates and targets. Curr. Alzheimer Res. *4*, 378–385.

van der Zee, J., Gijselinck, I., Van Mossevelde, S., Perrone, F., Dillen, L., Heeman, B., Bäumer, V., Engelborghs, S., De Bleecker, J., Baets, J., et al. (2017). TBK1 Mutation Spectrum in an Extended European Patient Cohort with Frontotemporal Dementia and Amyotrophic Lateral Sclerosis. Hum. Mutat. *38*, 297–309.

Wang, C., Deng, L., Hong, M., Akkaraju, G.R., Inoue, J., and Chen, Z.J. (2001). TAK1 is a ubiquitin-dependent kinase of MKK and IKK. Nature *412*, 346–351.

STAR★METHODS

KEY RESOURCES TABLE

REAGENT or RESOURCE	SOURCE	IDENTIFIER
Antibodies		
Anti-Cactus	S.A.Wasserman	AB_2314056
Anti-cleaved Caspase3	Abcam	AB_443014
Anti-diseased Tau	Abcam	AB_246808
Anti-Dorsal	Developmental Studies Hybridoma Bank (DSHB)	AB_528204
Anti-Fos	S. Sweeney (gift)	AB_11172288
Anti-Gfp	U.Mayor (gift)	N/A
Anti-Gfp	Abcam	AB_305643
Anti-Gfp	Molecular Probes	AB_221568
Anti-Ikk	S.Hayashi (gift)	N/A
Anti-Jra	S. Sweeney (gift)	AB_11164271
Anti-Ki67	DAKO	M7240
Anti-Ki67	Abcam	Ab833
Anti-Myc	Santa Cruz Biotechnology	AB_627268
Anti-NeuN	Millipore	AB_2298772
Anti-NeuN	Chemicon	MAB377
Anti-phosphoHistoneH3	Abcam	AB_304763
Anti-phosphoHistoneH3	Abcam	AB_443110
Anti-pIKK	S.Hayashi (gift)	N/A
Anti-Sim	S.Crews (gift)	N/A
Anti-Sim1	Thermo Fisher Scientific	PA5-113657
Anti-pTak1	Cell Signaling Technology	AB_330493
Anti-pTbk1	Cell Signaling	Cat.No. 5483
Anti-Tau	Abcam	AB_1281142
Anti-βtubulin	Developmental Studies Hybridoma Bank (DSHB)	AB_528499
Bacterial and virus strains		
Top10F	ThermoFisher Cat.No C303003	N/A
Biological samples		
Human postmortem brain sections (subiculum region)	Southwest Dementia Brain Bank	N/A
Chemicals, peptides, and recombinant proteins		
NBT/ BCIP	SigmaAldrich Cat No. 11681451001	N/A
Critical commercial assays		
TSA kit	Thermofisher Cat.No.B40953	N/A
Vectastain Elite ABC-Peroxidase kit	Vector Laboratories	AB_2336827
DAB Substrate Kit	Vector Laboratories	AB_2336382
Topo TA cloning kit	Thermofisher Cat.No.K450001	N/A
Experimental models: organisms/strains		
Wild type Oregon R-C	BDSC 5	BDSC_5
UAS-dl.H	BDSC9319	BDSC_9319
egrMI10187/ CyOTwi-GAL4/2xUAS-2EGFP	BDSC53467	BDSC_53467
egrMI10790/ CyOTwi-GAL4/2xUAS-2EGFP	BDSC55540	BDSC_55540

(*Continued on next page*)

Continued

REAGENT or RESOURCE	SOURCE	IDENTIFIER
UAS-egrRNAi	BDSC55276	BDSC_55276
UAS-human3RTau	BDSC78846	BDSC_78846
UAS-myr-GFP	BDSC32198	BDSC_32198
UAS-Traf6.S	BDSC58991	BDSC_58991
Tak1	BDSC26272	BDSC_26272
Ik2/ CyOTwi-GAL4/2xUAS-2EGFP	DGGR109663	DGGR_109663
UAS-Ik2-myc	DGGR109665	DGGR_109665
UAS-Ik2DN	DGGR109666	DGGR_109666
Rho-GAL4	Gift from C.Klaembt, (Klaes et al., 1994)	N/A
UAS-GFP-αtubulin62E	(Bossing et al., 2012)	N/A
Sim-GAL4	Gift from C.Klaembt, (Scholz et al., 1997)	N/A
UAS-human4RTau	Gift from M.Feany, (Fulga et al., 2007)	N/A
UAS-Toll10b-myc	Gift from T.Yp, (Hu et al., 2004)	N/A
Oligonucleotides		
5′ BAMH1-MyD88 full-length GGATCC-CGCCAAGTGCGAATGCGCCCT	SigmaAldrich	N/A
3′ Spe1-MyD88 truncated ACTAGT-CGGGTAGACATGTGTAGAGACCAG	SigmaAldrich	N/A
3′ Spe1-MyD88 ACTAGT-TCCGCCGGCCGTCTGCAGCTTGCT	SigmaAldrich	N/A
Software and algorithms		
Adobe Photoshop CS6	Adobe	N/A
Adobe Illustrator CS6	Adobe	N/A
Excel for Mac 16.16.12	Microsoft	N/A
https://astatsa.com/WilcoxonTest/	N/A	N/A
https://www.socscistatistics.com/tests/fisher/default2.aspx	N/A	N/A

RESOURCE AVAILABILITY

Lead contact

Further information and requests for resources and reagents should be directed to and will be fulfilled by the Lead Contact, Torsten Bossing (torsten.bossing@plymouth.ac.uk).

Materials availability

Fly strains generated during this study can be requested by emailing to the lead contact.

Data and code availability

All data reported in this paper will be shared by the lead contact upon request.

EXPERIMENTAL MODEL AND SUBJECT DETAILS

Fly stocks

From the Bloomington stock collection we obtained the following fly stocks:

UAS-dI.H (BDSC9319), egrMI10187/ CyOTwi-GAL4/2xUAS-2EGFP (BDSC53467), egrMI10790/ CyOTwi-GAL4/2xUAS-2EGFP (BDSC55540), UAS-egrRNAi (TRiP.HMC03963, BDSC55276), UAS-human3RTau (UAS-hMAPT.ON3R, BDSC78846), UAS-myr-GFP (BDSC32198), UAS-Traf6.S (BDSC58991), UAS-wgn.IR (BDSC58994), Tak1 (BDSC26272). From the Kyoto Stock Center we obtained Ik2/ CyOTwi-GAL4/2xUAS-2EGFP (DGGR109663), UAS-Ik2-myc (DGGR109665), UAS-Ik2DN (DGGR109666), Other fly lines we used are UAS-GFP-α-tubulin62E (Bossing et al., 2012), Oregon R, rho-GAL4 (Klaes et al., 1994), sim-GAL4 (Scholz et al., 1997), UAS-human3RTau, UAS-human4RTau (Fulga et al., 2007), UAS-Toll10b-myc (Hu et al., 2004).

Human post-mortem brain tissue

Formalin-fixed paraffin-embedded human brain tissue sections (8μm) were obtained from the Southwest Dementia Brain Bank Bristol under license HTA12273. Patient samples are age and gender balanced. Further details in Table S1.

METHOD DETAILS

Cell ablation and embryo injections

Embryos were prepared and desiccated as described previously (Bossing and Technau, 1994). Midline cell ablations were performed as described previously (Bossing et al., 2012) and carried out with an inverted microscope (Zeiss Axiovert) using a 63x oil immersion objective. Ablation capillaries have an outer diameter of approximately about 3μm and a tip bevelled at an angle of 25°. Briefly, using the capillary, the perivitelline membrane of *Drosophila* embryos was pierced along the posterior edge formed by its adhesion to the glue-coated coverslip. Great care was taken to avoid any contact between tissue and capillary in this preparatory steps. Using stage and micromanipulator control the capillary was steered inside the perivitelline space, above the midline. After the capillary tip reached the middle of the embryo, the tip was lifted into the midline and midline cells were slowly sucked into the capillary retracting the capillary at the same time. Ablations in *simG4>myrGFP* were performed under epifluorescence, maximal 30 s of excitation (480nm), using a LED source (CoolLED pE-100) and Zeiss filter set 10.

We injected 100ug/ ml of the microtubule depolymerizing drug vinblastine (Sigma, V1377) in 1%DMSO, or 1%DMSO in water into the perivitelline space of embryos as vehicle controls.

Time between manipulation of embryos and fixation after injection/ ablation varied between assays; 5 – 15min to test for protein phosphorylation and Dorsal nuclear entry, 30 - 45 min to analyze mitosis, to 60 - 120min to check for accumulation of newly synthesized proteins. Before fixation the Halocarbon oil covering the embryos was removed by squirting PBS with 0.4% Triton X-100 (PBT) out of a pulled Pasteur capillary alongside the glued down embryos. The same procedure was used to fix the embryos, spraying the samples with 4% formaldehyde in PBT out of a pulled Pasteur pipette. After 20min, samples were washed 3 times with PBS, and under PBS the vitelline membrane was removed manually. Embryos were transferred into watch glasses, fixed for 10min with 4% formaldehyde in PBS, washed and subjected to immunohistochemistry.

Immunohistochemistry

The following antibodies were used: anti-cactus (rabbit, 1:500, gift of SA. Wasserman), anti-cleaved Caspase-3 (rabbit, 1:50, Abcam 13847), anti-Cyclin B1 (mouse, 1:100; Novus Biological NB500), anti-diseased Tau (GT-38) (mouse, 1:100, abcam ab246808), anti-Dorsal (mouse, 1:100, Developmental Studies Hybridoma Bank 7A4), anti-Fos (rabbit, 1:1000, gift of S.Sweeney), anti-GFP (rabbit, 1:2000, gift of U. Mayor), anti-GFP (goat, 1:200, Abcam 6673), anti-Ik2 (mouse, 1:100(Oshima et al., 2006), anti-Jra (1:100, guinea-pig, gift of S. Sweeney), anti-Ki67 (mouse, DAKO m7246, 1:100), anti-Ki67 (rabbit, Abcam, ab833, 1:100), anti-Myc (mouse, 1:50, Santa Cruz Biotechnology A1209), anti-pHistoneH3 (S10) (rabbit, 1:2000, Abcam 5176), anti-pHistoneH3 (S10) (mouse, 1:200, Abcam 14955), anti-pIk2 (S175) (rabbit, 1:500(Otani et al., 2011), anti-NeuN (mouse, 1:100; Chemicon MAB377), anti-pTak1 (T187) (rabbit, 1:100, Cell Signaling Technology 4536), anti-pTbk1 (S172) (rabbit, 1:100, Cell Signaling Technology), anti-Sim (guinea pig, 1:500, gift of S. Crews), anti-Tau (mouse, 1:100, Abcam 805), anti-β-tubulin (mouse, 1:400, Developmental Studies Hybridoma Bank E7). All antibodies were diluted in PBT. Immunohistochemistry of *Drosophila* embryos was performed as described in Schmidt-Ott and Technau (1992). Embryos were incubated in 70% Glycerol overnight at 4°C, opened up to expose the ventral nerve cord/ ventral ectoderm with a dissecting needle and embedded in 70% Glycerol/ Vectashield (1/1). Images were recorded with a Leica SPE and a Leica SP8 confocal and level-adjusted, rotated, cut and assembled with Photoshop CS6.

Generation of MyD88 and MyD88DN transgenics

Previous studies showed that deletion of the N terminus of MyD88 (aa 1-236) generates a dominant negative construct blocking Toll signaling (Horng and Medzhitov, 2001). We generated this deletion and a full-length version of MyD88 by using the following primers to amplify cDNAs out of an embryonic cDNA pool:

5′ BAMH1-MyD88 full-length GGATCC-CGCCAAGTGCGAATGCGCCCT,
5′ Spe1-MyD88 truncated ACTAGT-CGGGTAGACATGTGTAGAGACCAG,
3′ MyD88 ACTAGT-TCCGCCGGCCGTCTGCAGCTTGCT.

Both constructs were cloned into pCR 2.1 Topo vector (Invitrogen) for sequencing. After confirmation of the sequence (SourceBioscience), the constructs were cloned into a pUASp vector which contained a C-terminal GFP in frame (kind gift of D. St Johnston). Constructs were injected into yw; P(ry, Δ2-3), Sb/TM6, Ubx embryos (Robertson et al., 1988).

Immunohistochemistry of human brain tissue and image analysis

Brain sections were deparaffinized in xylene (twice, 5min), rehydrated in serial dilutions of ethanol (2min each) and washed in H_2O (10min). Immunofluorescence staining was performed as described (Evans et al., 2018). Briefly, autofluorescent signal was quenched with 0.1% Sudan Black (Sigma-Aldrich, UK) in 70% ethanol (10min at room temperature, RT). Antigen retrieval performed by boiling sections in 10mM citrate buffer (pH 6.0) in a microwave oven (700 W, 30min), followed by wash in H_2O and equilibration in PBS (5 min). Sections were blocked with 5% normal goat serum (NGS) in PBS with 0.03% Triton X-100 (PBS-0.03%T; 1h RT) followed by incubation with primary antibodies in PBS-0.03%T (overnight, 4°C). Alexa Fluor conjugated secondary antibodies (1:300, Invitrogen Molecular Probes) were applied diluted in PBS-0.03%, 5% NGS (1h, RT). Sections were mounted in 1:1 of 70% glycerol/Vectashield

(Vector laboratories). Classical stainings followed published procedures (Evans et al., 2018; Garcia-Reitböck et al., 2010), with few modifications. Antigen retrieval was performed as above, followed by incubation in PBS-0.1%T with 3%H_2O_2 and 20% MeOH (30min, RT), washes in PBS and incubation in Bouin's solution (Sigma; 1min, RT). After washes in PBS, sections were blocked with 5%NGS in PBS-0.1%T (1h, RT) and incubated (overnight, 4°C) with the first primary antibody in PBS-0.1%T. Alkaline phosphatase (AP) conjugated secondary antibody (1:300; Sigma) was applied in PBS-0.1%T, 5% NGS (1h, RT). Sections were washed in detection buffer (50ml: 5ml 1M TRIS-HCl ph9.5; 2.5ml 1M MgCl; 50ul Tween) followed by incubation with NBT/BCIP in detection buffer according to manufacturer instructions (Roche). Signal development was stopped by washes with PBS-0.1%T. Sections were next blocked with 5%NGS in PBS-0.1%T (15min, RT) and incubated with the second primary antibody (overnight, 4°C). After washes, sections were incubated with biotinylated secondary antibodies (1:300, Vector Laboratories) for 2h at RT. ABC (Avidin-Biotin Complex) kit was used for signal amplification following manufacturer instructions (Vector Laboratories). Detection of signal was performed via conventional DAB/ H_2O_2 reaction (Vector Laboratories). Signal development was stopped by washes with PBS-0.1%T. Sections were subjected to a final fixation step (4% formaldehyde in PBS; 5min, RT) followed by PBS washes, and mounted using DPX histology mountant (Sigma). The specificity of stainings was controlled by omission of primary antibodies. Imaging was performed on a Leica IM8 microscope using LAS X software. Images were loaded into Fiji software and visual scoring of cells was conducted using the Cell Counter plugin. For each subiculum section analyzed, 6 random fields were scored totalling an area of 1.51mm^2. Mann-Whitney U statistical tests, following confirmation of non-parametric nature of the data, were employed using Sigma Plot software.

QUANTIFICATION AND STATISTICAL ANALYSIS

Statistical tests used, number of biological replicates/ samples, averages and p values are stated in figure texts. We used t tests for parametric data, Mann-Whitney U tests for non-parametric data and Fisher exact test for contingency tables. Software used were Excel for t test, Sigma Plot for Mann-Whitney U test and https://www.socscistatistics.com/tests/fisher/default2.aspx for Fisher Exact test. S.E.M, median and average are indicated in Graphs.